Active noise control without tap length selection: a model order weighting method

Yongjie Zhuang[1], Manan Mittal
Electrical & Computer Engineering, Stony Brook University
Light Engineering Lab, Stony Brook, New York 11794

Rashen Fernando, Ryan M. Corey
Discovery Partners Institute and University of Illinois Chicago
851 S. Morgan St., Chicago, Illinois 60607

Andrew C. Singer
College of Engineering and Applied Sciences, Stony Brook University
100 Engineering Bldg, Stony Brook, New York 11794

ABSTRACT

Conventional active noise control systems typically rely on fixed tap lengths in control filters. Determining an appropriate tap length is challenging, even within a straightforward time-invariant environment. This challenge is exacerbated when essential system responses, such as primary noise characteristics or primary path responses, remain partially unknown and necessitate the use of an adaptive filter. A trade-off emerges between convergence rate and steady-state performance when selecting a fixed tap length in adaptive filters. In time-varying environments, the optimal tap length may even dynamically shift over time. Thus, prior attempts have been made to introduce variable tap length algorithms to dynamically adapt tap length in real time. However, the performance of variable tap length algorithms can be sensitive to the choice of additional parameters and noise level. This paper exploits a model order weighting approach by combining the outputs of filters of different tap lengths based on their predicted noise control performance. This proposed method demands minimal additional prior information compared to the variable tap length methods. The noise control performance, as demonstrated by specific examples of active noise control, is presented and analyzed.

[1]yongjie.zhuang@stonybrook.edu

1. INTRODUCTION

Active noise control (ANC) functions by processing signals acquired from reference sensors, subsequently generating a control signal intended for secondary speakers to emit signals that act as anti-sound waves, attempting to mitigate noise levels within targeted noise control zones. The development of efficient digital signal processors and digital-to-analog/analog-to-digital chips paved the way for implementing ANC techniques in a wide range of applications [1] such as earphones [2–5], automobiles [6], HVAC systems [7–10], and ventilation windows [11, 12].

Conventional ANC systems typically rely on least mean square (LMS) methods with a fixed tap length (or model order). Even in a simple time-invariant environment where the essential system responses such as primary noise characteristics and primary path responses can be measured in advance, trial and error is usually involved to select an appropriate tap length. This challenge intensifies when primary noise characteristics and system responses are partially unknown or change over time, requiring the use of adaptive filters. A trade-off emerges between convergence rate and steady-state performance when using fixed tap lengths in adaptive filters. Although a long tap-length ANC filter can achieve better steady-state performance, it limits the maximum step size and convergence rate [13]. In time-varying environments, the mean-square error optimal tap length may even dynamically shift over time.

To address the abovementioned tap length selection challenge, variable tap length algorithms were developed to adaptively change tap length in real time [14–18]. For example, the Segmented Filter method [14, 16] partitions a long filter into several segments and adjusts the number of segments based on the output error levels; the gradient descent based method [15, 16] adapts the tap length along the negative gradient direction of the squared estimation error; the fractional tap-length method [16] allows pseudo fractional tap length to improve the robustness and computational complexity compared with other methods [16, 19]. However, the performance of variable tap length algorithms can be sensitive to the noise level [19, 20], step length, error width [21], input signal characteristics, and filter dimension [22]. Thus, prior knowledge of the statistics of the filtering scenario is needed to properly tune these methods [20]. Some variable step length methods may require additional assumptions such as a two-sided exponential decay envelope in the control filter's impulse response [18].

In contrast to the variable tap length methods, this paper describes a model order weighting approach that demands minimal additional prior information. This weighting strategy is based on the universal linear prediction methods described in [23, 24] that are twice universal, with respect to both the parameters and model orders. A universal approach concerning a set of candidate filters implies that the performance of this method is at least comparable (has a vanishing asymptotic regret) with respect to the best among those candidates. Usually, multiple candidate filters are implemented simultaneously and the output of the universal method is a combination of all candidate filters. Combining filters based on individual performance, known as a mixture of experts, has shown success in various ANC applications: using a combination of different fractional tap-length methods [19], step sizes [20, 25, 26], filter structures [27–31], cost functions [32], time and frequency domains FxLMS [33], among others. Although the computational burden can be higher than that of a single controller, this burden can be alleviated through multicore processors [34], digital twin architectures [35], as well and order-recursive methods, such as lattice filters [23].

Section 2 begins with an analytical examination demonstrating that the convergence rate of a long ANC filter is expected to be slower, thus laying the foundation for using different tap lengths. Subsequently, this section describes the proposed universal ANC tap length weighting method with a block diagram. In Section 3, the noise control performance is initially presented in a simple yet illustrative case. This preliminary case aligns with the analytical analysis, indicating that a larger tap length tends to result in a slower convergence rate. Furthermore, it showcases the effectiveness of the proposed universal tap length ANC algorithm. To evaluate the proposed method in a more realistic scenario, a simulated room response is generated. Results show that the proposed method achieves the best noise control performance at all time ranges. One of the pivotal assumptions in the proposed algorithm is the availability of an accurate secondary path estimation. Thus, an investigation of the robustness of the proposed method in instances where the estimated secondary path deviates from the true secondary path is also presented.

2. ALGORITHM

Figure 1(a) shows the block diagram of a conventional ANC system, in which $x[n]$ denotes the reference signal acquired by the reference microphone, H denotes the primary path from the reference microphone to the error microphone, G and $\hat{G}$ denote the true and estimated secondary path from the secondary (control) source to the error microphone, $\tilde{x}[n]$ denotes the reference signal $x[n]$ filtered by the estimated secondary path $\hat{G}$, $d[n]$ is the noise signal at the error microphone location to be canceled by the ANC system, and $e[n]$ is the noise signal after using the ANC system. Additionally, W is the control filter to be designed and the design objective is usually to minimize the power of $e[n]$. A common choice of W is filtered-x LMS algorithm (FxLMS) where W is a finite impulse response (FIR) filter and an appropriate pre-determined tap length M is required. Let the filter coefficients vector be $\vec{w}[n] = [w_0[n], w_1[n], \ldots, w_{M-1}[n]]^{\mathrm{T}}$, the filter output is

$$y[n] = \vec{w}[n]^{\mathrm{T}}\vec{x}[n], \tag{1}$$

where $\vec{x}[n] = [x[n], x[n-1], \ldots, x[n-M+1]]$. The FxLMS adaption rule is [36]:

$$\vec{w}[n+1] = \vec{w}[n] - \alpha\vec{r}[n]e[n], \tag{2}$$

where, $\vec{r}[n] = [\tilde{x}[n], \tilde{x}[n-1], \ldots, \tilde{x}[n-M+1]]^{\mathrm{T}}$ when $\hat{G} = G$, and $\alpha > 0$ is the step length.

Let $\mathbf{R}_{rr} = E\left[\hat{\vec{r}}[n]\vec{r}[n]^{\mathrm{T}}\right]$, where $\hat{\vec{r}}[n]$ is the estimate of $\vec{r}[n]$ and $\hat{\vec{r}}[n] = \vec{r}[n]$ if $\hat{G} = G$. To ensure convergence of FxLMS algorithm, α should satisfy $\alpha < 2/\lambda_{max}(\mathbf{R}_{rr})$ [36]. The convergence rate is proportional to $\alpha\lambda_{min}(\mathbf{R}_{rr})$ [37]. Thus, the convergence rate is linearly proportional to $\lambda_{min}(\mathbf{R}_{rr})/\lambda_{max}(\mathbf{R}_{rr})$. Using Cauchy's interlacing theorem (also known as the separation theorem) [38], we can show that a larger tap length M may result in a smaller convergence rate.

Lemma 2.1 *(Cauchy's interlacing theorem) Let $\mathbf{B} \in C^{m\times m}$ be a M-by-M Hermitian matrix and be the leading principal submatrix of Hermitian matrix $\mathbf{A} \in C^{(M+1)\times(M+1)}$. Then*

$$\lambda_1(\mathbf{A}) \leq \lambda_1(\mathbf{B}) \leq \lambda_2(\mathbf{A}) \leq \lambda_2(\mathbf{B}) \leq \cdots \leq \lambda_M(\mathbf{A}) \leq \lambda_M(\mathbf{B}) \leq \lambda_{M+1}(\mathbf{A}), \tag{3}$$

where λ_i denotes the i-th eigenvalue of a matrix in ascending order.

Using Lemma 2.1, clearly

$$\frac{\lambda_{min}(\mathbf{A})}{\lambda_{max}(\mathbf{A})} = \frac{\lambda_1(\mathbf{A})}{\lambda_{M+1}(\mathbf{A})} \leq \frac{\lambda_1(\mathbf{B})}{\lambda_M(\mathbf{B})} = \frac{\lambda_{min}(\mathbf{B})}{\lambda_{max}(\mathbf{B})}. \tag{4}$$

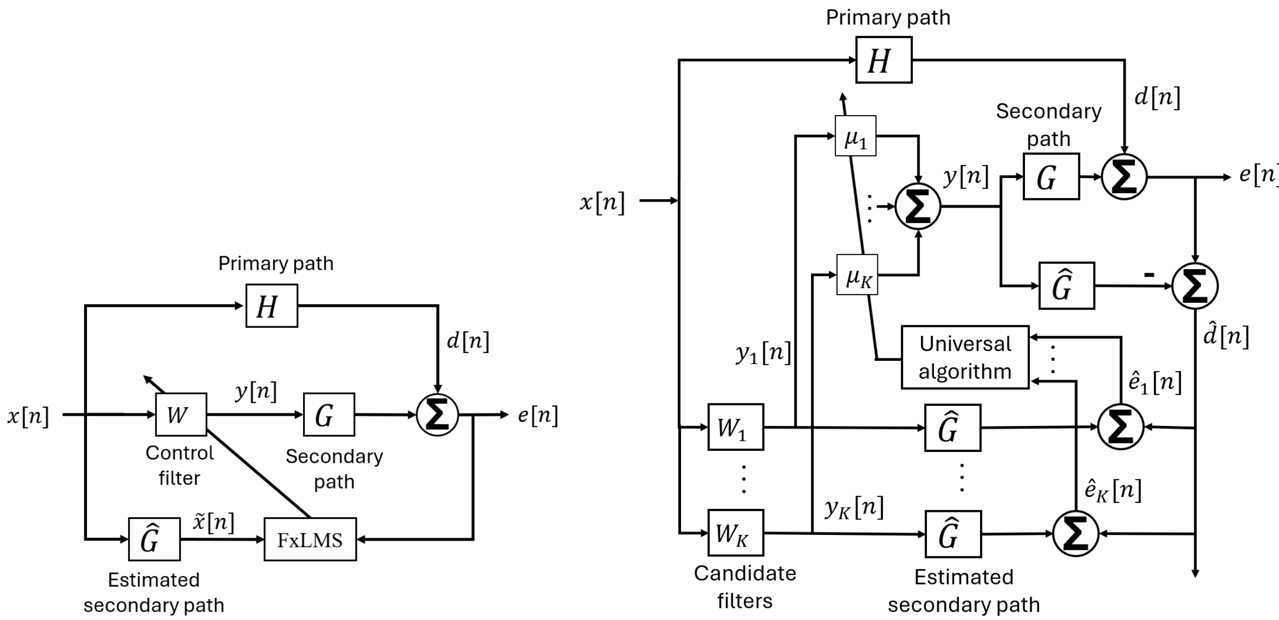

(a) (b)

Figure 1: Block Diagram of (a) conventional and (b) proposed algorithm in an ANC system. For brevity, the FxLMS adaption part in (b) is omitted when plotting the block diagram.

An M-by-M $\mathbf{R}_{rr}$ is the leading principal submatrix of a $(M+1)$-by-$(M+1)$ $\mathbf{R}_{rr}$ with one tap longer.Thus, a smaller tap length may have a larger eigenvalue ratio $\lambda_{min}(\mathbf{R}_{rr})/\lambda_{max}(\mathbf{R}_{rr})$ (i.e., faster convergence rate). However, it may have worse steady-state performance due to insufficient length.

In contrast to the conventional single filter structure, Figure 1(b) shows the proposed universal algorithm. K candidate filters $W_1, \ldots, W_K$ with tap lengths $M_1, \ldots, M_K$ respectively are used simultaneously in the ANC system. For brevity, the FxLMS adaption block for each candidate filter is omitted in the block diagram. Note that in real-time implementation, candidate filters cannot be directly implemented simultaneously in the physical world which prevents the availability of the ground truth of noise control performance of each candidate filter. To obtain the estimated noise control performance using each candidate filter, an estimated secondary path $\hat{G}$ is required to obtain the estimated noise signal of each candidate filter $\hat{e}_1[n], \ldots, \hat{e}_K[n]$. The outputs of each candidate filter are weighted and summed to form the input for control speaker $y[n]$:

$$y[n] = \sum_{k=1}^{K} \mu_k[n] y_k[n], \tag{5}$$

where $y_k[n]$ is the output of the k-th candidate control filter, μ_k is the mixture weights that are computed based on the performance-weighted combination as in [23]:

$$\mu_k[n] = \frac{\exp(-\frac{1}{2c}\ell_{n-1,k})}{\sum_{j=1}^{K} \exp(-\frac{1}{2c}\ell_{n-1,j})}, \tag{6}$$

where c is a design parameter that controls how responsive the universal algorithm is to the performance difference between different candidate filters; $\ell_{n-1,j}$ is the estimated cumulative noise power from time index 0 to $n-1$ when j-th candidate control filter is used. That is:

$$\ell_{n-1,j} = \gamma\ell_{n-2,j} + (1-\gamma)\hat{e}_j[n-1]^2 = (1-\gamma)\sum_{i=0}^{n-1}\gamma^{n-1-i}\,\hat{e}_j[i]^2, \tag{7}$$

where $0 < \gamma \leq 1$ is a forgetting factor so the cumulative noise power can track the time-varying environment.

3. RESULTS

In this section, a simple but illustrative case is first presented to demonstrate the basic principle of the proposed universal algorithm. Then the universal algorithm is applied to a more realistic simulated room response case considering both perfect and imperfect secondary path estimation. For all cases, design parameter $c = 0.01$ in Eq. (6) and forgetting factor $\gamma = 0.99$ in Eq. (7) are used. The step length for each fixed tap length filter is tuned to 1/3 of the convergence bound. 100 Monte Carlo simulations were implemented and the mean power is shown for all the noise control performance figures.

3.1. Simple Response Case

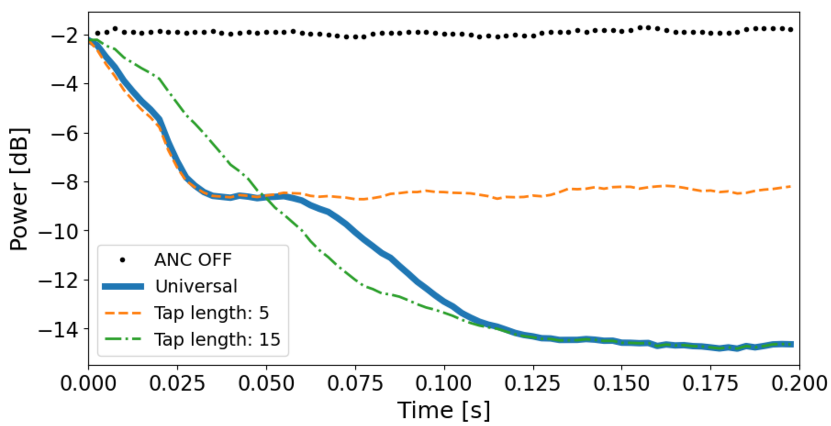

Figure 2: Noise power when using fixed tap lengths and the universal method in the simple response case. 100 Monte Carlo simulations were implemented and the mean power is shown.

Suppose the impulse response of the primary path is $H(z) = 1$ and the secondary path is $G(z) = 1 + 0.5z^{-10}$ in this simple response case. Then, the ideal optimal control filter $W^*(z)$ should be

$$W^*(z) = -\frac{H(z)}{G(z)} = -\frac{1}{1+0.5z^{-10}} = -1 + 0.5z^{-10} - 0.25z^{-20} + 0.125z^{-30} - \ldots \tag{8}$$

For perfect cancelation, an infinitely large tap length M should be used. Let's consider two different tap lengths: $M_1 = 5$ and $M_2 = 15$. Clearly, when tap length $M_1 = 5$ is used, only the first term -1 is included. And tap length $M_2 = 15$ can include the first and second terms $(-1 + 0.5z^{-10})$ which will achieve better steady-state performance.

To consider the convergence rate, suppose the input reference signal $x[n]$ is an i.i.d. standard Gaussian noise. When $x[n]$ is filtered by the secondary path $G(z) = 1 + 0.5z^{-10}$ to get $\tilde{x}[n]$,

$E[\tilde{x}[n]\tilde{x}[n-m]]$ is only non-zero when $m = 0, \pm 10$. Thus, when $M_1 = 5$ is used, $\mathbf{R}_{rr}$ is an identity matrix and $\lambda_{min}(\mathbf{R}_{rr})/\lambda_{max}(\mathbf{R}_{rr}) = 1$. When $M_1 = 15$ is used, $\lambda_{min}(\mathbf{R}_{rr})/\lambda_{max}(\mathbf{R}_{rr}) \approx 0.43 < 1$, which should have a slower convergence rate. This also confirms the analysis in Section 2 that a larger tap length has a negative impact on the eigenvalue ratio.

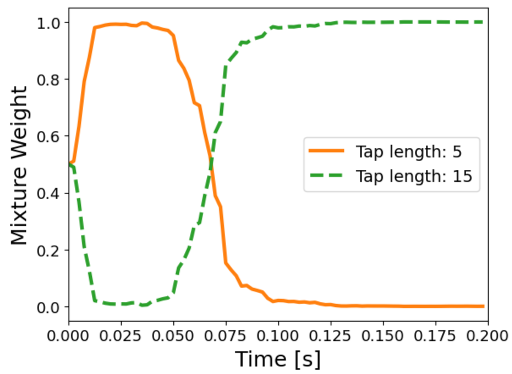

Figure 3: The mixture weights of two candidate tap lengths in the simple response case.

One hundred Monte Carlo simulations were implemented and the mean power is shown in Figure 2. Compared with the tap length $M_2 = 15$ filter, the tap length $M_1 = 5$ filter has a faster convergence rate at the early stage but worse steady-state performance, which aligns the analysis above. The universal algorithm can achieve both a faster convergence rate at the early stage and better steady-state performance. This shows the advantages of using the proposed universal algorithm. The mixture weights $\mu_k[n]$ shown in Figure 3 demonstrate that at the early stage tap length $M_1 = 5$ has a higher weight and at the later stage tap length $M_2 = 15$ has a higher weight. The transition starts around 0.05 s which aligns with the results shown in Figure 2.

3.2. Simulated Room Response Case

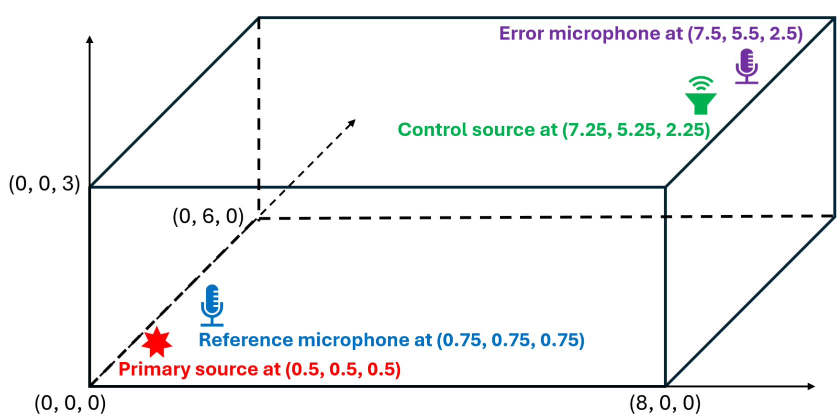

Figure 4: The dimension of the simulated room and the locations of the placed primary source, secondary (control) source, reference microphone, and error microphone. (unit: meter)

The simple response case in the previous subsection is illustrative but too simplified. To investigate the universal algorithm in a more realistic case, a room response is simulated using Pyroomacoustics package [39]. The room setup is shown in Figure 4. The plasterboard ceiling is on battens with a large air space above. The floor is fully covered with cotton carpet. One wall (south) is fully covered by tight velvet curtains and the other three walls are fully covered with Rockwool with a thickness of 50 mm and density of 40 kg/m^3. The maximum order of image sources is 10. The impulse responses of the transfer paths from noise source to reference microphone, from noise source to error microphone, and from secondary source to error microphone are shown in Figure 5. The reverberation time (60 dB) RT60 of this room is around 1 second.

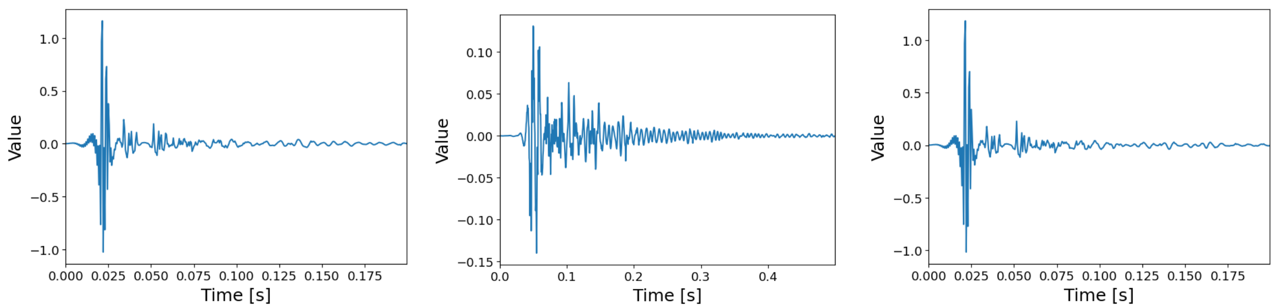

(a) (b) (c)

Figure 5: The impulse responses of transfer path (a) from noise source to reference microphone, (b) from noise source to error microphone, and (c) from secondary source to error microphone.

The noise control performance at the early stage (before 50 s) and the full range (0 - 300 s) are shown in Figure 6 (a) and (b) respectively. The trade-off between convergence rate and steady-state performance for three different fixed tap lengths (200, 400, and 800) can be clearly seen in both figures. The universal algorithm can closely track the best noise control performance among these three fixed tap length filters. The mixture weights are shown in Figure 7.

3.3. Noisy Secondary Path Estimation Case

One strong assumption in the proposed universal algorithm for ANC is that the estimated secondary path $\hat{G}$ is a perfect model of the true secondary path G, i.e., $\hat{G} = G$. This estimated secondary path is important as it is required in both the FxLMS algorithms and also in universal algorithms to get the estimated cumulative noise power. In realistic applications, perfect secondary path estimation is unlikely. This subsection investigates the robustness of the proposed universal algorithm when the estimated secondary path is not the same as the true secondary path.

The room responses in the previous subsection are again used as the true responses. Similarly, 100 Monte Carlo simulations are implemented. In each Monte Carlo simulation, the estimated secondary path is randomly perturbed, i.e., $\hat{G} = G + v$, where v is an i.i.d. zero-mean Gaussian random process and the power of v equals 30% of the power of G. So the estimated secondary path can be considered as a noisy version of the true secondary path with a signal-to-noise ratio of around 5 dB. The noise control performance under this secondary path perturbation is shown in Figure 8. Compared with Figure 6, Figure 8 shows that the noise control performance will be negatively affected for the fixed tap length case (especially for tap length of 800) because of the mismatch between estimated and true secondary paths. Nevertheless, the universal algorithm can still closely track the best performance among these three candidate filters at all times. This demonstrates the robustness of the proposed universal algorithm. The mixture weights are shown in Figure 9 which also align with the results in Figure 8.

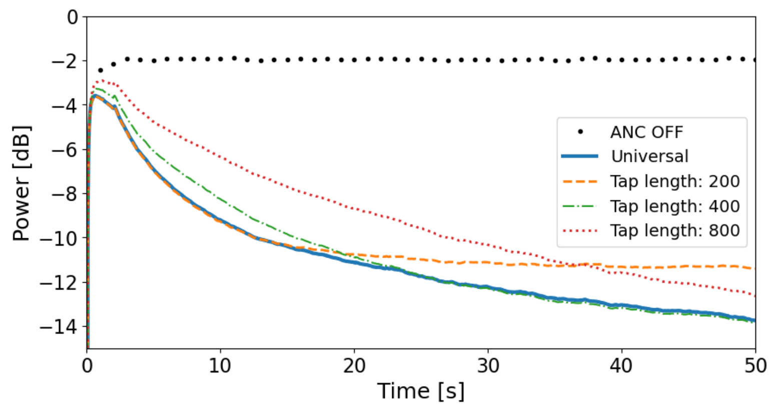

(a)

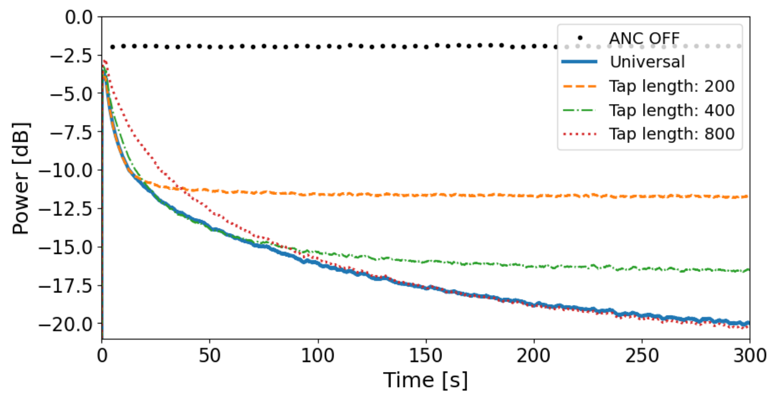

(b)

Figure 6: Noise power when using fixed tap lengths and the universal method in the simulated room response case (a) before 50 s and (b) from 0 to 300 s. 100 Monte Carlo simulations were implemented and the mean power is shown.

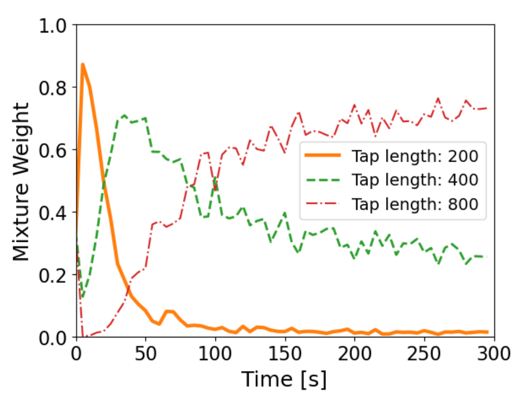

Figure 7: The mixture weights of three candidate tap lengths in the simulated room response case.

4. CONCLUSIONS

The trade-off between the convergence rate and steady-state performance is inevitable when using fixed tap length ANC filters. The analysis shows that a smaller tap length tends to have a faster

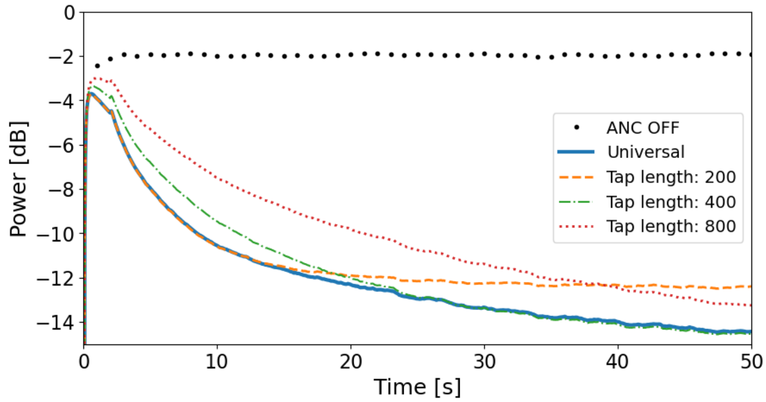

(a)

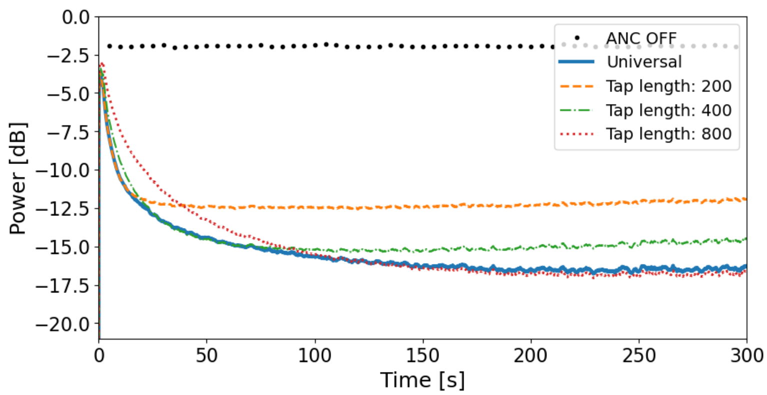

(b)

Figure 8: Noise power when using fixed tap lengths and the universal method in the 30% randomly perturbed simulated room response case (a) before 50 s and (b) from 0 to 300 s. 100 Monte Carlo simulations were implemented and the mean power is shown.

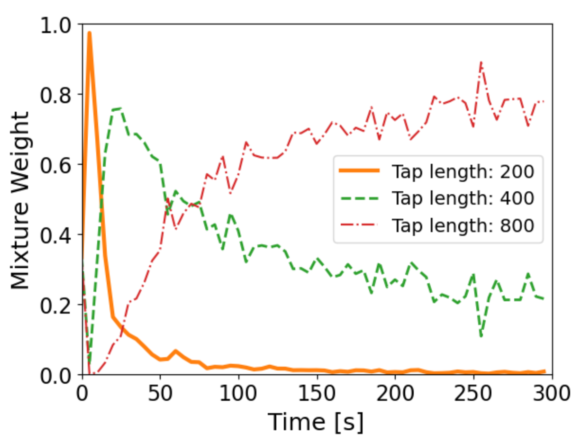

Figure 9: The mixture weights of three candidate tap lengths in the 30% randomly perturbed simulated room response case.

convergence rate, motivating the use of a smaller tap length in the early transient period and a larger tap length when approaching the steady state period. The proposed universal ANC method implements multiple candidate filters with different tap lengths simultaneously and weights their outputs for the control speaker (i.e., the mixture of experts). Results show the proposed method can effectively achieve the best noise control performance among all the candidate filters at all time ranges, even when there is a mismatch between the estimated and true secondary paths.

It is important to note that the proposed universal algorithm can be naturally extended beyond the use of different tap length candidate filters. For example, universal over different step sizes or step size scheduling, filter types, adaptive and non-adaptive filters, different subspace dimensions in the improved Wiener Filter solution [40], among other variations.

ACKNOWLEDGEMENTS

The authors acknowledge support from the Foxconn Interconnect Technology sponsored Center for Networked Intelligent Components and Environments (C-NICE) at the University of Illinois at Urbana-Champaign.

REFERENCES

[1] Dongyuan Shi, Bhan Lam, Woon-Seng Gan, Jordan Cheer, and Stepehen J Elliott. Active noise control in the new century: The role and prospect of signal processing. In *INTER-NOISE and NOISE-CON Congress and Conference Proceedings*, volume 268, pages 5141–5151. Institute of Noise Control Engineering, 2023.

[2] Cheng-Yuan Chang, Antonius Siswanto, Chung-Ying Ho, Ting-Kuo Yeh, Yi-Rou Chen, and Sen M. Kuo. Listening in a noisy environment: Integration of active noise control in audio products. *IEEE Consumer Electronics Magazine*, 5(4):34–43, 2016.

[3] Sen M Kuo, Yi-Rou Chen, Cheng-Yuan Chang, and Chien-Wen Lai. Development and evaluation of light-weight active noise cancellation earphones. *Applied Sciences*, 8(7):1178, 2018.

[4] Yongjie Zhuang and Yangfan Liu. A stable IIR filter design approach for high-order active noise control applications. In *Acoustics*, volume 5, pages 746–758. MDPI, 2023.

[5] Yongjie Zhuang and Yangfan Liu. A constrained optimal hear-through filter design approach for earphones. In *INTER-NOISE and NOISE-CON congress and conference proceedings*, volume 263, pages 1329–1337. Institute of Noise Control Engineering, 2021.

[6] Prasanga N Samarasinghe, Wen Zhang, and Thushara D Abhayapala. Recent advances in active noise control inside automobile cabins: Toward quieter cars. *IEEE Signal Processing Magazine*, 33(6):61–73, 2016.

[7] Koki Shige, Naoyuki Takeda, and Osamu Terashima. Research on the active noise control technology for the reduction of the air conditioner noise in a vehicle cabin. In *INTER-NOISE and NOISE-CON Congress and Conference Proceedings*, volume 268, pages 6179–6186. Institute of Noise Control Engineering, 2023.

[8] Yongjie Zhuang and Yangfan Liu. Constrained optimal filter design for multi-channel active noise control via convex optimization. *The Journal of the Acoustical Society of America*, 150(4):2888–2899, 2021.

[9] Yongjie Zhuang and Yangfan Liu. A numerically stable constrained optimal filter design method for multichannel active noise control using dual conic formulation. *The Journal of the Acoustical Society of America*, 152(4):2169–2182, 2022.

[10] Yongjie Zhuang, Zhuang Mo, and Yangfan Liu. Warmstarting strategies for convex optimization based multi-channel constrained active noise control filter design. *Noise Control Engineering Journal*, 71(5):332–343, 2023.

[11] Bhan Lam, Stephen Elliott, Jordan Cheer, and Woon-Seng Gan. Physical limits on the performance of active noise control through open windows. *Applied Acoustics*, 137:9–17, 2018.

[12] Hsiao Mun Lee, Yuting Hua, Zhaomeng Wang, Kian Meng Lim, and Heow Pueh Lee. A review of the application of active noise control technologies on windows: Challenges and limitations. *Applied Acoustics*, 174:107753, 2021.

[13] Dah-Chung Chang and Fei-Tao Chu. Feedforward active noise control with a new variable tap-length and step-size filtered-x LMS algorithm. *IEEE/ACM Transactions on Audio, Speech, and Language Processing*, 22(2):542–555, 2014.

[14] F Riera-Palou, James M Noras, and DGM Cruickshank. Linear equalisers with dynamic and automatic length selection. *Electronics Letters*, 37(25):1, 2001.

[15] Yuantao Gu, Kun Tang, and Huijuan Cui. LMS algorithm with gradient descent filter length. *IEEE Signal Processing Letters*, 11(3):305–307, 2004.

[16] Yu Gong and Colin FN Cowan. An LMS style variable tap-length algorithm for structure adaptation. *IEEE Transactions on Signal Processing*, 53(7):2400–2407, 2005.

[17] Ningning Liu, Yuedong Sun, Yansong Wang, Hui Guo, Bin Gao, Tianpei Feng, and Pei Sun. Active control for vehicle interior noise using the improved iterative variable step-size and variable tap-length LMS algorithms. *Noise Control Engineering Journal*, 67(6):405–414, 2019.

[18] Dah-Chung Chang and Fei-Tao Chu. A new variable tap-length and step-size FxLMS algorithm. *IEEE Signal Processing Letters*, 20(11):1122–1125, 2013.

[19] Yonggang Zhang and Jonathon A Chambers. Convex combination of adaptive filters for a variable tap-length LMS algorithm. *IEEE Signal Processing Letters*, 13(10):628–631, 2006.

[20] Miguel Ferrer, Alberto Gonzalez, Maria de Diego, and Gema Pinero. Convex combination filtered-x algorithms for active noise control systems. *IEEE Transactions on audio, speech, and language processing*, 21(1):156–167, 2012.

[21] Yufei Han, Mingjiang Wang, and Yun Lu. Variable tap-length algorithm with mixed parameter. *Applied Sciences*, 8(6):939, 2018.

[22] Asutosh Kar, Trideba Padhi, Banshidhar Majhi, and MNS Swamy. Analysing the impact of system dimension on the performance of a variable-tap-length adaptive algorithm. *Applied Acoustics*, 150:207–215, 2019.

[23] A.C. Singer and M. Feder. Universal linear prediction by model order weighting. *IEEE Transactions on Signal Processing*, 47(10):2685–2699, 1999.

[24] A. C. Singer, S. S. Kozat, and M. Feder. Universal linear least squares prediction: upper and lower bounds. *IEEE Transactions on Information Theory*, 48(8):2354–2362, August 2002.

[25] Haiquan Zhao, Xiangping Zeng, Zhengyou He, Shujian Yu, and Badong Chen. Improved functional link artificial neural network via convex combination for nonlinear active noise control. *Applied Soft Computing*, 42:351–359, 2016.

[26] Yabing Cheng, Chao Li, Shuming Chen, Pingyu Ge, and Yuntao Cao. Active control of impulsive noise based on a modified convex combination algorithm. *Applied Acoustics*, 186:108438, 2022.

[27] Fernando Basilio Felix, Max de Castro Magalhaes, and Guilherme de Souza Papini. Improved active noise control algorithm based on the convex combination method. *Journal of the Brazilian Society of Mechanical Sciences and Engineering*, 43:1–12, 2021.

[28] Ning Yu, Zhaoxia Li, Yinfeng Wu, Renjian Feng, and Bin Chen. Convex combination-based active impulse noise control system. *Journal of Low Frequency Noise, Vibration and Active Control*, 39(1):190–202, 2020.

[29] Lei Wang, Kean Chen, and Jian Xu. Convex combination of the fxapv algorithm for active impulsive noise control. *Mechanical Systems and Signal Processing*, 181:109443, 2022.

[30] J Rodríguez, I Ibarra, E Pichardo, JG Avalos, and JC Sánchez. Convex combination of fxecap–fxeclms algorithms for active noise control. In *2018 IEEE International Autumn Meeting on Power, Electronics and Computing (ROPEC)*, pages 1–6. IEEE, 2018.

[31] Nithin V George and Alberto Gonzalez. Convex combination of nonlinear adaptive filters for active noise control. *Applied Acoustics*, 76:157–161, 2014.

[32] Pucha Song and Haiquan Zhao. Filtered-x generalized mixed norm (fxgmn) algorithm for active noise control. *Mechanical Systems and Signal Processing*, 107:93–104, 2018.

[33] Trideba Padhi, Mahesh Chandra, Asutosh Kar, and MNS Swamy. A new hybrid active noise control system with convex combination of time and frequency domain filtered-x lms algorithms. *Circuits, Systems, and Signal Processing*, 37:3275–3294, 2018.

[34] Alberto Gonzalez, Miguel Ferrer, Maria de Diego, Carles Roig, and Gema Piñero. Convex combination strategies for active noise control on multicore processors. In *Proceedings of the 17th International Congress on Sound and Vibration (ICSV 17), Cairo, Egypt*, pages 18–22, 2010.

[35] Chuang Shi, Feiyu Du, and Qianyang Wu. A digital twin architecture for wireless networked adaptive active noise control. *IEEE/ACM Transactions on Audio, Speech, and Language Processing*, 30:2768–2777, 2022.

[36] S.J. Elliott. *Signal Processing for Active Control*, chapter 3 - Single-Channel Feedforward Control, pages 103–175. Academic Press, 2001.

[37] S.J. Elliott. *Signal Processing for Active Control*, chapter 2 - Optimal and Adaptive Digital Filters, pages 49–102. Academic Press, 2001.

[38] Roger A. Horn and Charles R. Johnson. *Matrix Analysis*, chapter Hermitian Matrices, Symmetric Matrices, and Congruences, pages 225–312. Cambridge University Press, 2013.

[39] Robin Scheibler, Eric Bezzam, and Ivan Dokmanić. Pyroomacoustics: A python package for audio room simulation and array processing algorithms. In *2018 IEEE international conference on acoustics, speech and signal processing (ICASSP)*, pages 351–355. IEEE, 2018.

[40] Yongjie Zhuang, Xuchen Wang, and Yangfan Liu. Singular vector filtering method for mitigation of disturbance enhancement in multichannel active noise control systems. *Noise Control Engineering Journal*, 69(5):451–459, 2021.